Title

Origins of the Endo and Exo Selectivities in Cyclopropenone, Iminocyclopropene, and Triafulvene Diels–Alder Cycloadditions

Journal

The Journal of Organic Chemistry, 83(6)

ISSN

0022-3263

Authors

Levandowski, Brian J
Hamlin, Trevor A
Helgeson, Roger C
et al.

Publication Date

2018-03-16

DOI

10.1021/acs.joc.8b00025

Peer reviewed

HHS Public Access

Author manuscript

J Org Chem. Author manuscript; available in PMC 2019 January 02.

Published in final edited form as:

J Org Chem. 2018 March 16; 83(6): 3164–3170. doi:10.1021/acs.joc.8b00025.

Origins of the *Endo* and *Exo* Selectivities in Cyclopropenone, Iminocyclopropene, and Triafulvene Diels-Alder Cycloadditions

Brian J. Levandowski[#†], **Trevor A. Hamlin**[#‡], **Roger C. Helgeson**[†], **F. Matthias Bickelhaupt**[‡,§], and **K N. Houk**[†]

[†] Department of Chemistry and Biochemistry, University of California, Los Angeles, California 90095, United States [‡] Department of Theoretical Chemistry and Amsterdam Center for Multiscale Modeling (ACMM), Vrije Universiteit Amsterdam, 1081 HV Amsterdam, The Netherlands [§] Institute for Molecules and Materials (IMM), Radboud University, 6525 AJ Nijmegen, The Netherlands

[#] These authors contributed equally to this work.

Abstract

The endo and *exo* stereoselectivities of Diels—Alder reactions of cyclopropenone, iminocyclopropene, and substituted triafulvenes with butadiene were rationalized using density functional theory calculations. When cyclopropenone is the dienophile, there is a 1.8 kcal/mol preference for the *exo* cycloaddition with butadiene, while the reaction of 3-difluoro-methylene triafulvene with butadiene favors the *endo* cycloaddition by 2.8 kcal/mol. The influence of charge transfer and secondary orbital interactions on the stereoselectivity of Diels—Alder reactions involving triafulvenes and heteroanalogs is discussed. The predicted stereoselectivity correlates with both the charge and highest occupied molecular orbital (HOMO) coefficient at the C_3 carbon of the triafulvene motif.

Graphical Abstract

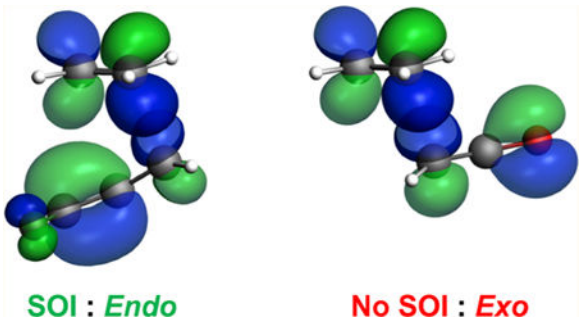

ASSOCIATED CONTENT

Supporting Information

The Supporting Information is available free of charge on the ACS Publications website at DOI: 10.1021/acs.joc.8b00025. Additional computational results, Cartesian coordinates, and energies of all stationary points (PDF)

Notes

The authors declare no competing financial interest.

1. INTRODUCTION

In 1969, Breslow reported that the Diels-Alder reaction of cyclopropenone with 1,3-diphenylisobenzofuran proceeds with unusual *exo* stereoselectivity (Scheme 1).[1] Berson reinvestigated this reaction in 1994 and confirmed the *exo*-selectivity of cyclopropenone with 1,3-diphenylisobenzofuran by obtaining the crystal structures of the *endo* and *exo* Diels-Alder adducts. Analysis of the reaction kinetics at −30 °C revealed an estimated preference of 50:1 *exo/endo.*

Bachrach computationally analyzed the Diels-Alder reaction between cyclopropenone and furan at the MP2 level.[3] He computed a 1.8 kcal/mol kinetic and a 6.4 kcal/mol thermodynamic preference for the *exo* adduct. The *exo* preference was attributed to a stabilizing electrostatic interaction between the oxygen atom of furan and the carbonyl carbon of the cyclopropenone in the *exo* transition state (Scheme 2).[3] Recently, we computed that cyclopropenone also reacts with *exo* stereoselectivity when cyclopentadiene is the diene,[4] in contrast to the highly *endo* selective cyclopropene.[5] This discovery, and the fact that cyclopropenones have emerged as stable, minimally invasive probes for bioorthogonal labeling studies,[6] prompted us to systematically study the origins of the *endo* and *exo* Diels-Alder stereoselectivity of cyclopropenone (l), cyclopropenethione (2), iminocyclopropene (4), the iminium derivative (3), and triafulvenes (5-7), with butadiene (Bd) (Scheme 3).

2. COMPUTATIONAL METHODS

Computations were carried out with *Gaussian* 09, revision D.01.[7] Geometry optimizations and vibrational frequency calculations were performed using the M06-2X[8] density functional with the 6-31+G(d) basis set. Single-point energies were calculated at the M06-2X/6-311++G(d,p) level of theory. The M06-2X functional has been shown to provide relatively accurate energies for cycloadditions[9]. Solvation effects of dichloromethane (DCM) were included in the optimizations and single-point energies using the self-consistent reaction field (SCRF) using the CPCM model.[10] Normal mode analysis was used to verify each stationary point as either a first-order saddle point or a minimum. The thermal corrections were computed from unscaled M06-2X/6-31+G(d) frequencies for a 1 M standard state and 298.15 K. Truhlar's quasiharmonic correction was applied by setting all positive frequencies below 100 cm^{-1} to 100 cm^{-1}.[11] The molecular orbital coefficients from the outer Gaussian function charges were calculated from natural bond orbital (NBO) analysis at the HF/6-31G(d)//CPCM-(DCM)-M06-2X/6-31+G(d) level of theory.[12]

Insight into the origins of the *endo* and *exo* stereoselectivity was provided by the distortion/interaction-activation strain model (D/I- ASM).[13] This analysis was performed using the ADF.2016.102 program[14] at the M06-2X/TZ2P[8,15] level of theory on the geometries optimized at CPCM-(DCM)-M06-2X/6-31+G(d) in *Gaussian 09.* In this framework, the potential energy surface in solution $\Delta E_{solution}(\zeta)$ is decomposed along the reaction coordinate ζ into the energy of the solute $\Delta E_{solute}(\zeta)$, specifically the reaction system in vacuum with the solution phase geometry, plus the solvation energy $\Delta E_{solvation}(\zeta)$.[16]

$$\Delta E_{\text{solution}}(\zeta) = \Delta E_{\text{solute}}(\zeta) + \Delta E_{\text{solvation}}(\zeta) \quad 1$$

Next, the intrinsic energy of the solute $\Delta E_{\text{solute}}(\zeta)$ is separated into the strain $\Delta E_{\text{strain}}(\zeta)$ associated with deforming the individual solute reactants, plus the interaction $\Delta E_{\text{int}}(\zeta)$ between the deformed solute reactants.

$$\Delta E_{\text{solute}}(\zeta) = \Delta E_{\text{strain}}(\zeta) + \Delta E_{\text{int}}(\zeta) \quad 2$$

The $\Delta E_{\text{int}}(\zeta)$ between the reactants is further analyzed by an energy decomposition analysis (EDA) in the conceptual framework provided by the Kohn—Sham molecular orbital (KS-MO) model[17] and is decomposed into three physically meaningful terms:

$$\Delta E_{\text{int}}(\zeta) = \Delta V_{\text{elstat}}(\zeta) + \Delta E_{\text{pauli}}(\zeta) + \Delta E_{\text{oi}}(\zeta) \quad 3$$

The $\Delta V_{\text{elstat}}(\zeta)$ term corresponds to the classical electrostatic interaction between unperturbed charge distributions, $\Delta E_{\text{Pauli}}(\zeta)$ is responsible for any steric repulsion, and the $\Delta E_{\text{oi}}(\zeta)$ accounts for charge transfer (HOMO—LUMO interactions) and polarization.

3. RESULTS AND DISCUSSION

Figure 1 shows the *endo* and *exo* transition states for the Diels—Alder reactions of butadiene (**Bd**) with triafulvenes (1-7). The computed activation free energies ($\Delta G^{\ddagger}$) are shown below each structure, in kcal/mol. For the *endo* and *exo* Diels—Alder reactions with Bd, the activation free energies are in the range 21-29 and 20-27 kcal/mol, respectively. The stereoselectivities of the triafulvene cycloadditions range from a 1.8 kcal/mol *exo* preference to a 2.8 kcal/mol *endo* preference. The cycloaddition of **Bd** with cyclopropenone (l) favors the *exo* approach by 1.8 kcal/mol, whereas the 3-difluoromethylene triafulvene (7) cycloaddition favors the *endo* reaction by 2.8 kcal/mol. The activation free energies for neutral triafulvene analogs range from 21.8 to 28.6 and from 24.4 to 26.8 in the *endo* and *exo* reactions, respectively. The activation free energies for the positively charged iminium cyclopropene (3) with a low lying lowest unoccupied molecular orbital (LUMO) energy are 20.5 and 19.5 for the *endo* and *exo* transition states, respectively.

The effect of each exocyclic cyclopropene group on the stability of 1-7 was assessed using the isodesmic reaction shown in Figure 2, which relates the stability of the triafulvene to a similarly substituted cyclopropane. All of the groups stabilize the cyclopropene to a greater extent than they stabilize the cyclopropane. We call this aromatic stabilization energy (ASE) since the substituted cyclopropenes have cyclic, potentially aromatic conjugation in the three-membered ring. A more positive number represents greater stability of the substituted cyclopropene compared to the substituted cyclopropane. Schleyer has shown that effects of

resonance and hyper-conjugation are also included in this isodesmic equation.[18] The substituents have a strong influence on the stability of the cyclopropene. For triafulvenes 1-7, the calculated aromatic stabilization enthalpies (ASE) are all stabilizing and range from 4.2 to 26.2 kcal/mol. The variation in stabilization arises primarily from differences in the aromaticity of the unsaturated three-membered ring. Electronegative substituents polarize the exocyclic double bond away from the cyclopropene ring, which causes the cyclopropene rings of these compounds to more closely resemble the 2π electron aromatic cyclopropenylium cation. The π-donor F destabilizes the triafulvene motif by increasing the four-electron character, thus decreasing the aromatic character of the cyclopropene ring.

The Diels—Alder reactions of **Bd** with cyclopropenes (1-7) are exergonic by −41 to −63 kcal/mol. Consistent with the Hammond postulate, the timing of the transition structures generally becomes earlier as the reaction is more exergonic. As shown in Figure 3a, there is no correlation between the activation enthalpies and the aromatic stabilization enthalpies (2, 3, and 5 are outliers). Figure 3b shows that there is a linear correlation between the exothermicity of reaction $(\Delta H_{\mathrm{rxn}})$ and the aromatic stabilization energy of the triafulvene. The substituents have a significant effect on the reaction free energy, by stabilizing the reactants, but have little effect on the product or on the activation energies.

Application of the distortion/interaction-activation strain model (D/I-ASM) provided quantitative insight into the origins of the reactivity differences and *endo* and *exo* stereoselectivity.[13] Figure 4a shows the results of our analysis for the *endo* (black) and *exo* (red) Diels-Alder reactions of **Bd** with 3-difluoro-methylene triafulvene (7). The strain, or distortion, curves are nearly identical along the respective reaction coordinates, and the *endo* selectivity is a result of the differences in the interaction energies. Figure 4b shows the decomposition of the interaction energy for the *endo* (black) and *exo* (red) Diels-Alder reactions of **Bd** with 7 along the reaction coordinate. The Pauli repulsion and electrostatic terms are nearly identical along the reaction coordinate. The differences in the strength of the orbital interactions in the *endo* and *exo* reactions are responsible for the *endo* Diels-Alder stereoselectivity of 7.

The results from the distortion/interaction-activation strain model along the reaction coordinate for the *endo* (black) and *exo* (red) Diels-Alder reactions of **Bd** with cyclopropenone (1) are shown in Figure 5a. The strain curves are nearly identical for the *endo* and *exo* reactions, and the *exo* stereoselectivity results from differences in interaction energies. Figure 5b shows the decomposition of the interaction energies into the electrostatic, Pauli repulsion and orbital components along the IRC. The *exo* selectivity of cyclopropenone (l) results from the combination of the electrostatic and orbital interactions, which overrule the *endo* preference of the Pauli repulsion and favor the *exo* transition state.

Figure 6 summarizes the NBO charges at the C_3 position of the triafulvene and heteroatom analogs 1-7, along with the sum of charges across all atoms of **Bd**, and the C_3 p-orbital coefficient of the triafulvene HOMO in the *endo* transition states. Secondary orbital interactions (SOI) involve overlap of the C_2 and C_3 p-orbitals of the **Bd** LUMO with the C_3 p-orbital of the cyclopropene HOMO in the endo transition state. The C_3 p-orbital coefficients in the HOMO of 1—7 range from 0.0 to 0.26. The charges at the C_3 position of

1—7 range from —0.18 to 0.61. Polarization of the exocyclic π-bond diminishes the π-electron density at the C_3 position and weakens the strength of the SOI. 3-Difluoromethylene has the largest p-orbital coefficient and the most negative charge at C_3 and is the most *endo* selective. Cyclopropenone (1) with the smallest p-orbital HOMO coefficient and the strongest positive charge at the C_3 is the most *exo* selective.

We next performed molecular orbital analyses to quantify the contribution of the SOI in the *endo* reactions of 1 and 7 with **Bd** (Figure 7). The molecular orbital (MO) diagrams and overlaps were calculated at the M06-2X/TZ2P//CPCM-(DCM)-M06-2X/6-31+g(d) level of theory by using Kohn—Sham[19] MO analyses on the geometries at C C bond forming distances of 2.24 Å. In the Diels—Alder reaction of 7 with **Bd**, the FMO energy gap ($\Delta\varepsilon$ = 6.3 eV) and the orbital overlap (S = 0.25) of HOMO(**Bd**)—LUMO(7) interaction are the same for the *endo* and *exo* transition states. The HOMO(7)—LUMO(**Bd**) interaction includes the effects of the SOIs in the *endo* transition state. The HOMO(7)—LUMO(Bd) of the *endo* and *exo* transition states both exhibit gaps with $\Delta\varepsilon$ = 6.4 eV. The orbital overlap of the HOMO(7)—LUMO(**Bd**) in the *endo* transition state (S = 0.17) is significantly greater than that in the *exo* transition state (S = 0.11), a result of the SOI that arises from the overlap of the p-orbital at the C_3 position in the HOMO of 7 with the C_2 and C_3 p-orbitals in the LUMO of **Bd** in the *endo* transition state.

The reaction between **Bd** and 1 proceeds primarily through a normal electron-demand Diels—Alder cycloaddition, where the key FMO interaction is between the HOMO(**Bd**)—LUMO(l) with an FMO energy gap of 6.3 eV for both the *endo* and *exo* approach (Figure 8). The orbital overlaps are similar for the *endo* and *exo* approach with overlaps of 0.24 and 0.25, respectively. The lower lying HOMO—1(l) interacts with the LUMO(**Bd**); however, this interaction has a relatively large energy gap of 9.1 eV for both the *endo* and *exo* cycloadditions. The orbital overlaps for the *endo* and *exo* approach are similar at 0.16 and 0.15, respectively. Similar orbital overlap of the HOMO—1 of 1 with the LUMO of **Bd** in the *endo* and *exo* transition state is evidence of weak secondary orbital interactions in the *endo* transition state. The weak SOIs with 1 are a result of the poor overlap between the small p-orbital coefficient at the C_3 position in the HOMO of 1 with the p-orbitals of the newly forming π-bond in the LUMO of **Bd**. Weak SOI explains why the *endo* selectivity disappears from 7 to 1, but does not explain why cyclopropenone is *exo* selective.

The charge transfer between the triafulvene and **Bd** also appears in the orbital interaction term. The charge at the C_3 position of the triafulvene and heteroatom analogs 1—7 ranges from —0.18 to 0.61 in the *endo* transition states (Figure 6). The reactions are normal electron-demand Diels—Alder reactions, and **Bd** becomes partially positively charged as a result of charge transfer to the dienophile. The magnitude of the charge transfer generally increases as the dienophile becomes more electron-deficient. The sum of charge across all the atoms of **Bd** ranges from 0.05 to 0.22 in the *endo* transition states of 1—7. Figure 9 shows a qualitative representation of a charge transfer interaction between the C_3 position of the triafulvene and **Bd** in the *endo* transition states. The charge transfer in the *endo* transition state can be understood as being more stabilizing when the C_3 carbon is negatively charged and destabilizing when the C_3 carbon is positively charged. Due to the increased distance between the C_3 position and the diene, this interaction is much weaker in the *exo* transition

state. The lack of secondary orbital interactions and the unfavorable charge transfer between the electropositive **Bd** fragment and the electropositive C_3 position of cyclopropenone (1) in the *endo* transition state explains why there is a preference for the *exo* transition state in the Diels—Alder reaction of **Bd** with cyclopropene (1).

We have previously shown that both secondary orbital and electrostatic interactions play a role in determining the *endo* and *exo* Diels—Alder stereoselectivity in reactions of 3-substituted cyclopropenes.[5b] The charge at the C_3 position of the cyclopropene correlates with the cyclopropene stereoselectivity in the absence of steric effects and serves as a useful way to predict the stereoselectivity of cyclopropene Diels—Alder reactions. Figure 10 shows a linear correlation between the stereoselectivity $\left(\Delta G^{\ddagger}_{\text{endo}} - \Delta G^{\ddagger}_{\text{exo}}\right)$ and the NBO charge at the C_3 position of the triafulvene for the Diels—Alder reactions of triafulvenes 1—7 with **Bd**. The stereoselectivity increases linearly with increasing positive charge at the C_3 position of 1—7 with cyclopropenethione 2, an obvious outlier, represented by the unfilled diamond.

The **π**-densities and charges at the C_3 positions are determined by the polarization of the exocyclic double bond. Compared to the C=O double bond of cyclopropenone (1), the C=S double bond of the cyclopropenethione (2) is less polarized because of the smaller difference in the electronegativities of carbon and sulfur compared to that of carbon and oxygen. However, sulfur is a strong **π** acceptor, and because of its size, it can accommodate additional **π**-electron density compared to oxygen. Theoretical studies by Wiberg et al. found that the **π**-densities of the C=O bond in cyclopropenone and the C=S bond in cyclopropenethione are similar, despite the differences in the polarization of the C=S of C=O bonds.[20] This is consistent with 1 and 2 having similarly small HOMO orbital coefficients at the C_3 carbon, but different charges at the C_3 carbon (see Figure 6).

Figure 11 shows the distortion/interaction—activation strain and energy decomposition analyses for the *endo* and *exo* Diels—Alder reaction of **Bd** with cyclopropenethione (2). The slightly *exo* stereoselectivity in the Diels—Alder reaction of **Bd** with 2 results from poor stabilization of the *endo* transition state through secondary orbital and electrostatic interactions.

4. CONCLUSIONS

The reactivities and stereoselectivities of Diels—Alder reactions of cyclopropenone and triafulvene analogs are controlled by both the charge and HOMO coefficient at the C_3 carbon. In the *endo* transition state, polarization of the exocyclic bond by electron-withdrawing groups weakens the strength of the stabilizing secondary orbital interactions and creates unfavorable charge transfer between the electropositive C_3 position of the triafulvene and butadiene that favors exo stereoselectivity. The Diels—Alder reactivities of the triafulvene and heteroanalogs decrease as the size of the HOMO coefficient at the C_3 carbon decreases as a result of weaker secondary orbital and charge transfer interactions. We predict that exo stereoselectivity is favored when the exocyclic triafulvene group is O, S, or NR_2^+, endo stereoselectivity when CR_2 is the exocyclic group, and poor stereoselectivity when NR is the exocyclic substituent.

Supplementary Material

Refer to Web version on PubMed Central for supplementary material.

ACKNOWLEDGMENTS

This work was supported by the National Science Foundation (NSF CHE-1361104), the National Institute of Health (NIH R01GM109078), and The Netherlands Organization for Scientific Research (NWO) through the Planetary and Exo-Planetary Science program (PEPSci) and the Dutch Astrochemistry Network (DAN). We thank the University of California, Los Angeles Institute for Digital Research and SURFsara for use of the Hoffman 2 and Cartesius computers, respectively. We also thank Dr. Ashay Patel and Dr. Pier Alexandre Champagne for helpful discussions and Prof. Claude Y. Legault for developing CYLview,[21] which was used to generate images of the optimized structures.

REFERENCES

(1). Breslow R; Ryan G; Groves JTJAm. Chem. Soc. 1970, 92, 988.

(2). Cordes MHJ; de Gala S; Berson JJAm. Chem. Soc. 1994,116, 11161.

(3). Bachrach SM J. Org. Chem. 1995, 60, 4395.

(4). Paton RS; Kim S; Ross AG; Danishefsky SJ; Houk KN Angew. Chem., Int. Ed. 2011, 50, 10366.

(5). (aWiberg KB; Bartley WJ J. Am. Chem. Soc. 1960, 82, 6375.(b)Levandowski BJ; Houk KNJAm. Chem. Soc. 2016,138, 16731.(c)Levandowski BJ; Hamlin TA; Bickelhaupt FM; Houk KN J. Org. Chem. 2017, 82, 8668. [PubMed: 28712288]

(6). (a) Shih H-W.; Prescher JA J.Am. Chem. Soc. 2015,137, 10036. [PubMed: 26252114] (b)Row R D.; Alexander AT; Mehl RA; Prescher JA; Shih H-W J. Am. Chem. Soc. 2017, 139, 7370. [PubMed: 28478678]

(7). Frisch MJ; Trucks GW; Schlegel HB; Scuseria GE; Robb MA; Cheeseman JR; Scalmani G; Barone V; Mennucci B; Petersson GA; Nakatsuji H; Caricato M; Li X; Hratchian HP; Izmaylov AF; Bloino J; Zheng G; Sonnenberg JL; Hada M; Ehara M; Toyota K; Fukuda R; Hasegawa J; Ishida M; Nakajima T; Honda Y; Kitao O; Nakai H; Vreven T; Montgomery JA, Jr.; Peralta JE; Ogliaro F; Bearpark M; Heyd JJ; Brothers E; Kudin KN; Staroverov VN; Kobayashi R; Normand J; Raghavachari K; Rendell A; Burant JC; Iyengar SS; Tomasi J; Cossi M; Rega N; Millam MJ; Klene M; Knox JE; Cross JB; Bakken V; Adamo C; Jaramillo J; Gomperts R; Stratmann RE; Yazyev O; Austin AJ; Cammi R; Pomelli C; Ochterski JW; Martin RL; Morokuma K; Zakrzewski VG; Voth GA; Salvador P; Dannenberg JJ; Dapprich S; Daniels AD; Farkas O; Foresman JB; Ortiz JV; Cioslowski J; Fox DJ Gaussian 09, revision D.01; Gaussian, Inc.: Wallingford, CT, 2009.

(8). Zhao Y; Truhlar DG Theor. Chem. Acc. 2008, 120, 215.

(9). (a) Pieniazek S; Houk KN Angew. Chem., Int. Ed. 2006,45,1442.(b)Pieniazek S; Clemente FR; Houk KN Angew. Chem., Int. Ed. 2008, 47, 7746.

(10). (a) Barone V; Cossi M J. Phys. Chem. A 1998, 102, 1995.(b)Cossi M; Rega N; Scalmani G; Barone VJ Comput. Chem. 2003, 24, 669.

(11). Zhao Y; Truhlar DG Phys. Chem. Chem. Phys. 2008, 10, 2813. [PubMed: 18464998]

(12). (a) Foster JP; Weinhold F J. Am. Chem. Soc. 1980, 102, 7211.(b)Reed AE; Weinhold FJ Chem. Phys. 1985, 83, 1736.(c)Reed AE; Weinstock RB; Weinhold FJ Chem. Phys. 1985, 83, 735. (d)Reed AE; Curtiss LA; Weinhold F Chem. Rev. 1988, 88, 899.

(13) (a). Bickelhaupt FM; Houk KN Angew. Chem., Int. Ed. 2017, 56, 10070.(b)Wolters LP; Bickelhaupt FM WIRES Comput. Mol. Sci. 2015, 5, 324.(c)Fernandez I; Bickelhaupt FM Chem. Soc. Rev. 2014, 43, 4953. [PubMed: 24699791] (d)van Zeist W-J; Bickelhaupt FM Org. Biomol. Chem. 2010, 8,3118. [PubMed: 20490400] (e)Ess DH; Houk KNJAm. Chem. Soc. 2008, 130, 10187.(f)Ess DH; Houk KN J. Am. Chem. Soc. 2007, 129, 10646. [PubMed: 17685614] (g)Bickelhaupt FM J. Comput. Chem. 1999, 20, 114.

(14). (a) te Velde G; Bickelhaupt FM; Baerends EJ; Fonseca Guerra C; van Gisbergen SJA; Snijders JG; Ziegler T Chemistry with ADF. J. Comput. Chem. 2001, 22, 931.(b)Fonseca Guerra C;

Snijders JG; te Velde G; Baerends EJ Theor. Chem. Acc. 1998, 99, 391.(c)ADF 2016, SCM Theoretical Chemistry; Vrije Universiteit, Amsterdam, The Netherlands, http://www.scm.com.

(15). (a) van Lenthe E; Baerends EJJ Comput. Chem. 2003, 24, 1142. (b) Franchini M; Philipsen PHT; van Lenthe E; Visscher LJ Chem. Theory Comput. 2014, 10, 1994.

(16). (a) Laloo JZA; Rhyman L; Ramasami P; Bickelhaupt FM; de Cozar A Chem. - Eur. J. 2016, 22,4431. [PubMed: 26879231] (b)Hamlin TA; van Beek B; Wolters LP; Bickelhaupt FM Chem. - Eur. J. 2018, 24, DOI: 10.1002/chem.201706075.

(17). (a) Ziegler T; Rauk A Inorg. Chem. 1979,18, 1755.(b)Ziegler T; Rauk A Inorg. Chem. 1979, 18, 1558.(c) Bickelhaupt FM; Nibbering NMM; Van Wezenbeek EM; Baerends EJ J. Phys. Chem. 1992, 96,4864.(d) Baerends EJ; Gritsenko OV J. Phys. Chem. A 1997, 101, 5383.

(18). (a) Schleyer P. v. R.; Puhlhofer F Org. Lett. 2002, 4, 2873. [PubMed: 12182577] (b) Wang Y; Fernandez I; Duvall M; Wu JI-C; Li Q; Frenking G; Schleyer P. v. J. Org. Chem. 2010, 75, 8252.

(19). (a) Bickelhaupt FM; Baerends EJ In Reviews in Computational Chemistry; Lipkowitz KB, Boyd DB, Eds.; Wiley-VCH: New York, 2000; Vol. 15, pp 1–86.(b)van Meer R; Gritsenko OV; Baerends EJJ Chem. Theory Comput. 2014, 10, 4432.

(20). (a) Wiberg KB; Rablen PR J.Am. Chem. Soc. 1995,117,2201.(b)Wiberg KB; Marquez MJ Am. Chem. Soc. 1998, 120, 2932.

(21). Legault CY, CYLview, 1.0b; Sherbrooke, QC: Universite de SherbrookeCanada, Sherbrooke, QC, 2009 Available at: http://www. cylview.org.

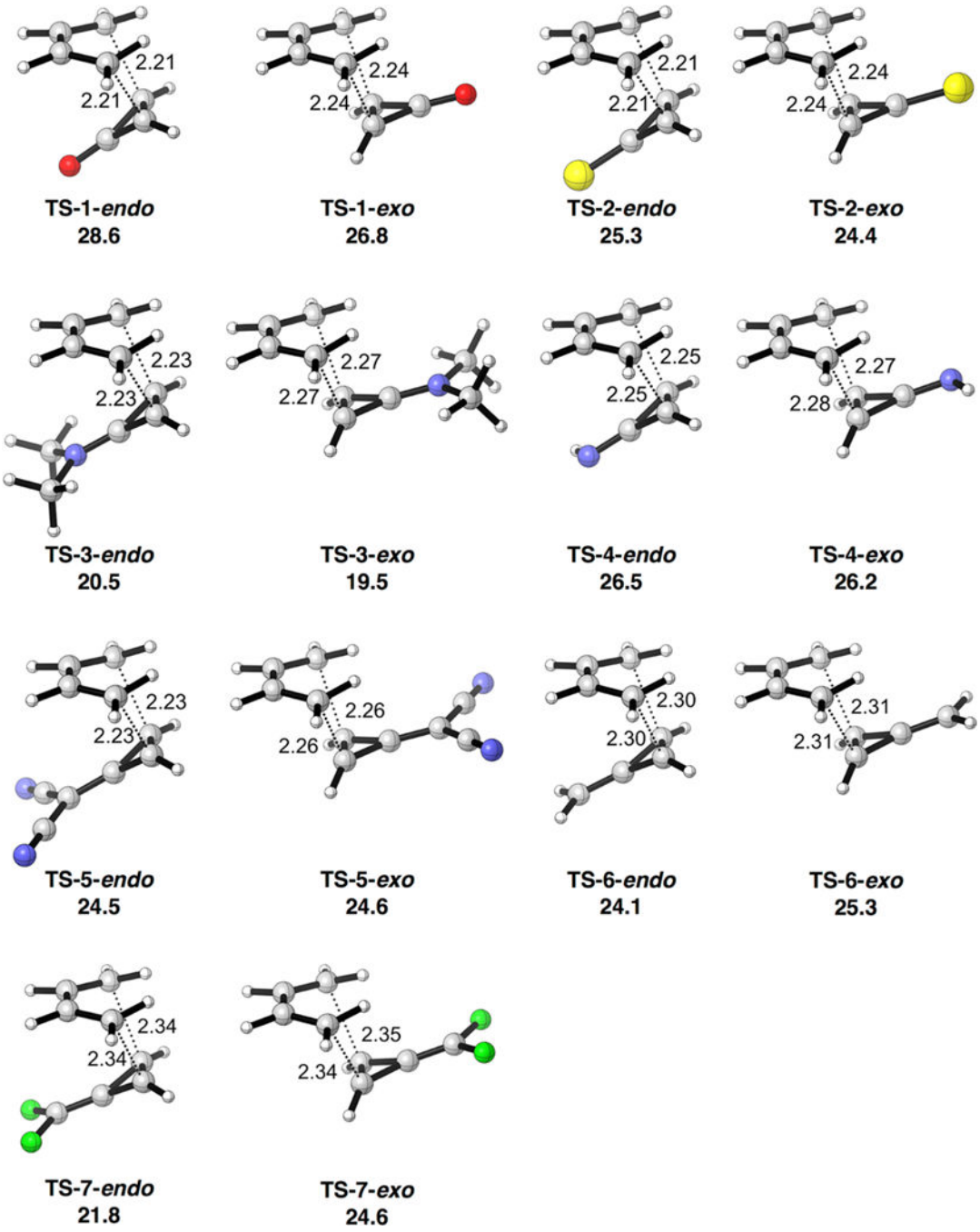

Figure 1.

Computed Diels—Alder transition structures for the reactions of butadiene (**Bd**) with triafulvenes 1—7. The two forming bond lengths are reported in angstroms, and activation free energies $\Delta G^{\ddagger}$ are reported in kcal/mol.

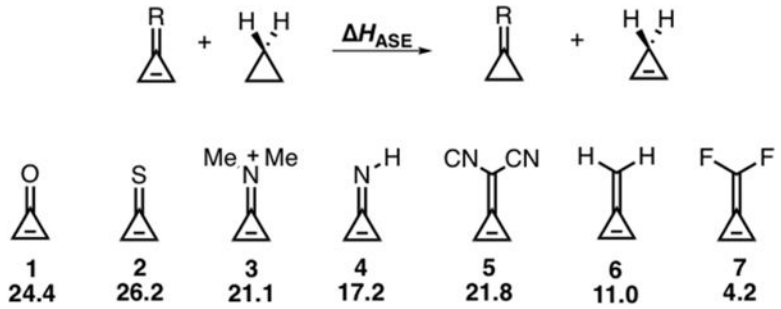

Figure 2.

Isodesmic equation relating the stability of substituted cyclopropenes (triafulvenes) to substituted cyclopropanes with the computed reaction enthalpies (ΔH_{ASE}) of triafulvenes 1-7 in the above isodesmic equation.

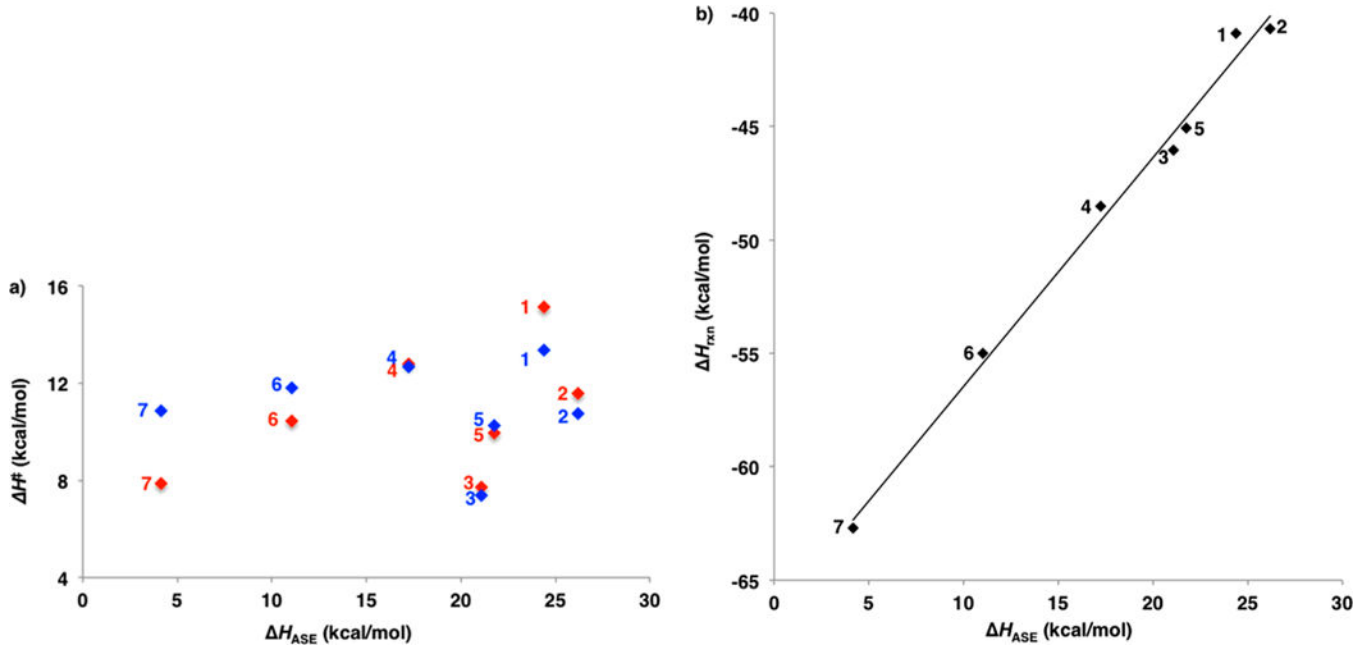

Figure 3.

(a) Plot of the activation enthalpies ($\Delta H^{\ddagger}$) of the Diels-Alder reactions of 1-7 with butadiene (**Bd**) versus the aromatic stabilization enthalpies (ΔH_{ASE}) (blue *endo*, red *exo*). (b) Plot of the reaction enthalpies (ΔH_{rxn}) versus the aromatic stabilization enthalpies (ΔH_{ASE}) for the Diels- Alder reactions of 1-7 with butadiene (**Bd**) ($\Delta H_{rxn} = 1.00\ \Delta H_{ASE} - 66.5$, $r^2 = 0.99$).

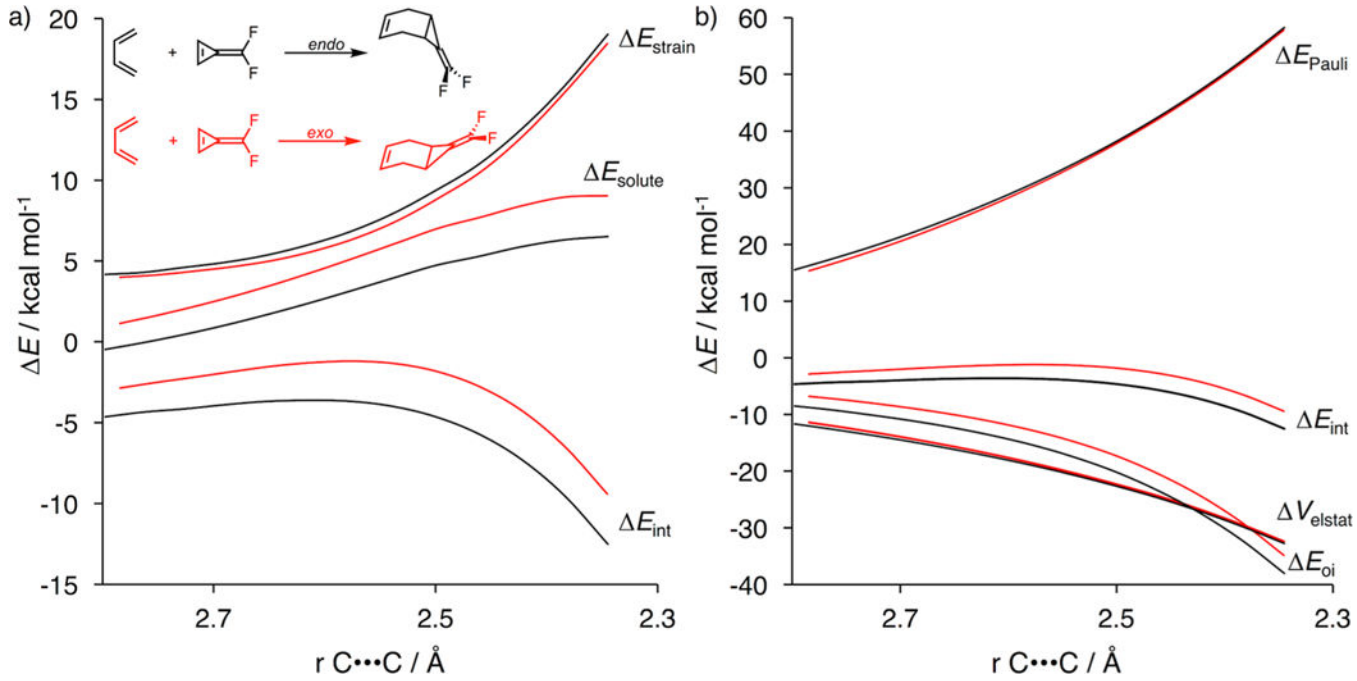

Figure 4.

(a) Distortion/interaction−activation strain and (b) energy decomposition analyses of the *endo* (black) and *exo* (red) cycloaddition reactions of butadiene (**Bd**) with 3-difluoromethylene triafulvene (7).

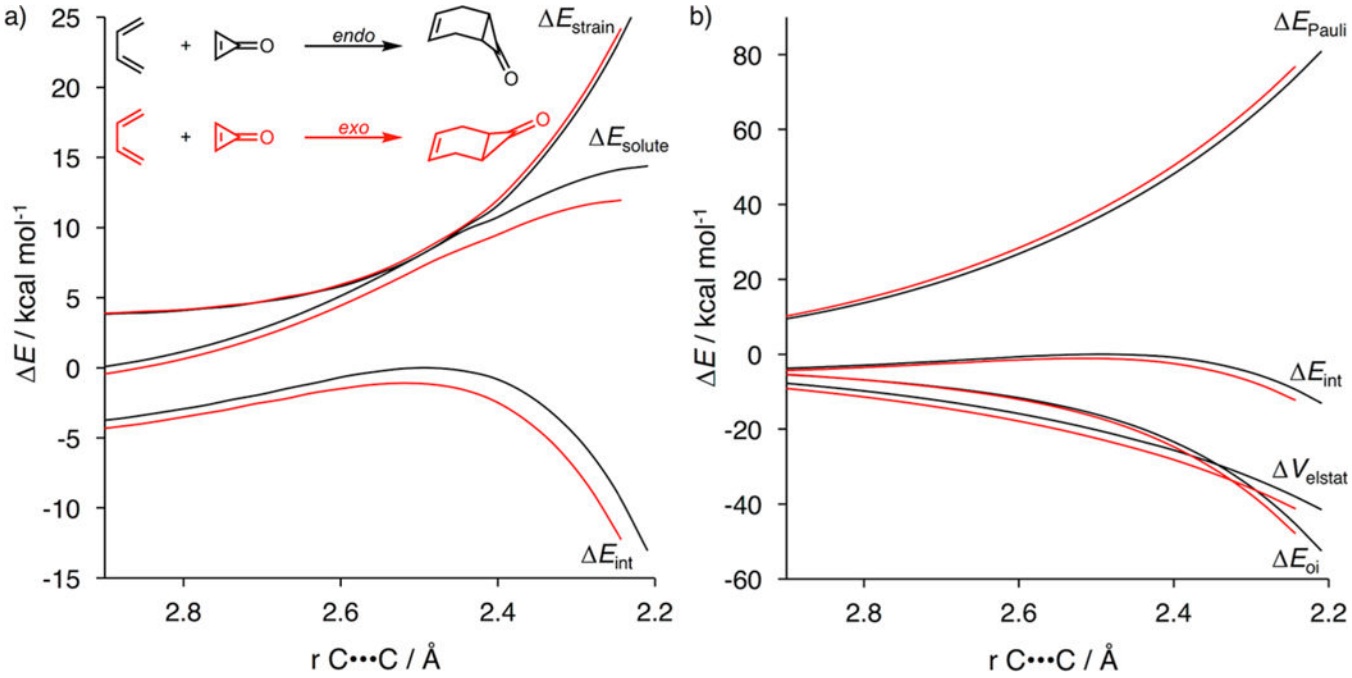

Figure 5.

(a) Distortion/interaction-activation strain and (b) energy decomposition analyses of the *endo* (black) and *exo* (red) cycloaddition reactions ofbutadiene (**Bd**) with cyclopropenone (1).

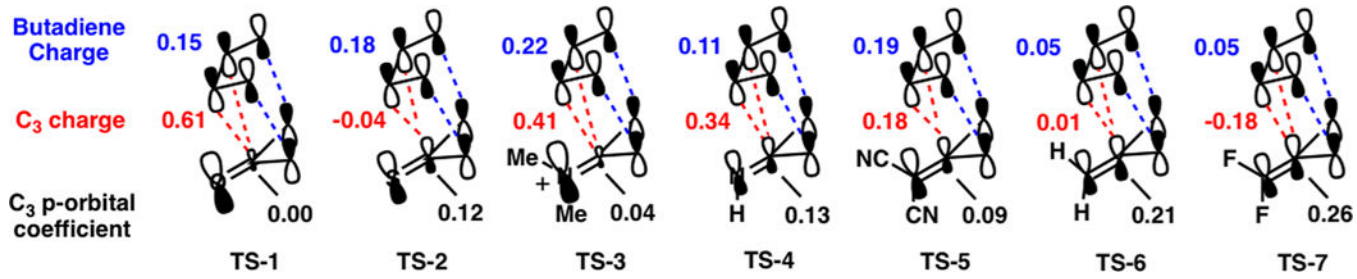

Figure 6.

Sum of charges across the butadiene (**Bd**) atoms, charge at the C_3 position of the triafulvene, and the C_3 p-orbital coefficient of the triafulvenes and heteroanalogs HOMO obtained from the *endo* transition state structures for triafulvenes 1-7. Primary orbital interactions and secondary orbital interactions are represented by blue and red lines, respectively.

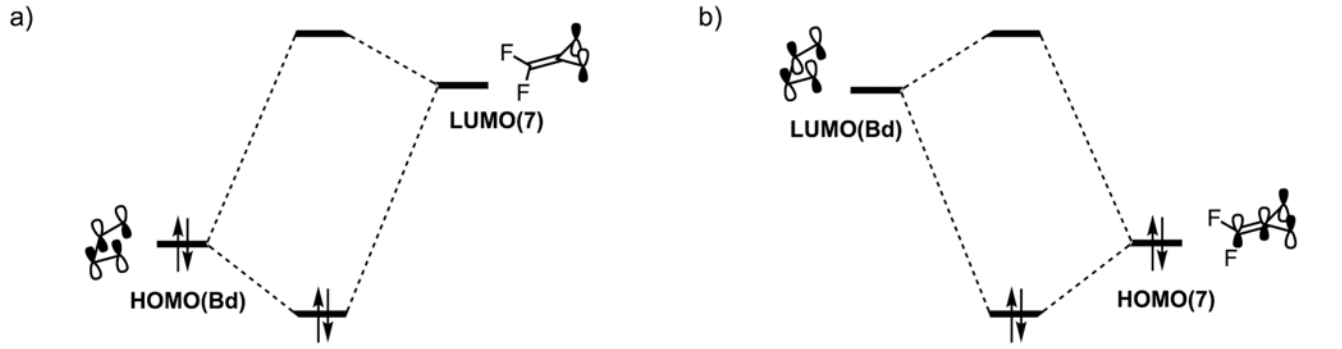

	Δε HOMO(Bd)–LUMO(7) (eV)	Orbital Overlap (S)
endo	6.3	0.25
exo	6.3	0.25

	Δε HOMO(7)–LUMO(Bd) (eV)	Orbital Overlap (S)
endo	6.4	0.17
exo	6.4	0.11

Figure 7.

MO diagram with orbital energy gap and overlap of (a) the HOMO(**Bd**)−LUMO(7) interaction and (b) the HOMO(7)−LUMO(Bd) for the cycloaddition between butadiene (**Bd**) and 3,3-difluoromethylene triafulvene (7), computed on structures with C···C bond forming distances of 2.24 Å.

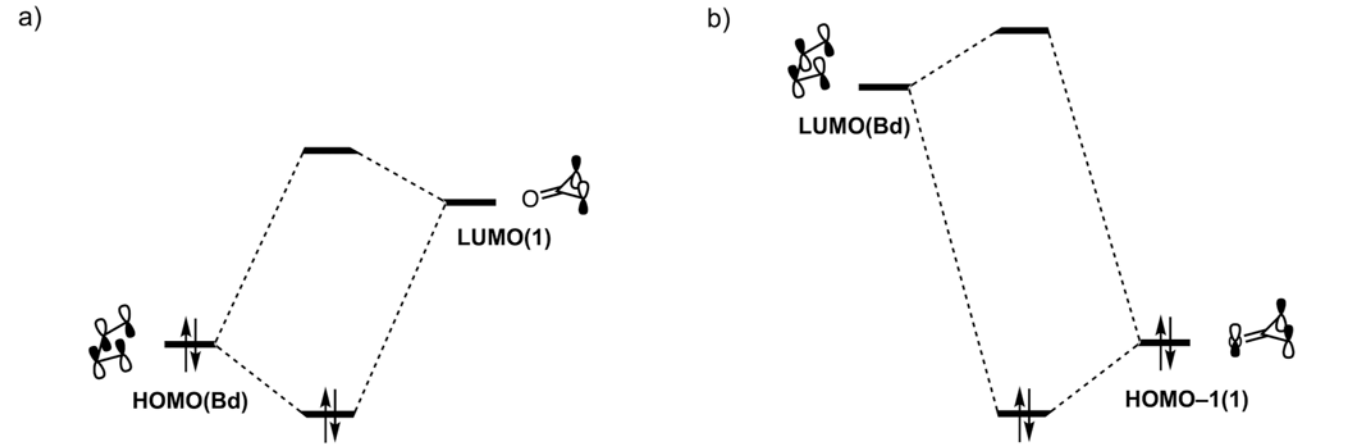

	Δε HOMO(Bd)–LUMO(1) (eV)	Orbital Overlap (S)
endo	6.3	0.24
exo	6.3	0.25

	Δε HOMO–1(1)–LUMO(Bd) (eV)	Orbital Overlap (S)
endo	9.1	0.16
exo	9.1	0.15

Figure 8.

MO diagram with orbital energy gap and overlap of the HOMO(**Bd**)−LUMO(1) interaction for the cycloaddition between butadiene (**Bd**) and cyclopropenone (1), computed on structures with C···C bond forming distances of 2.24 Å.

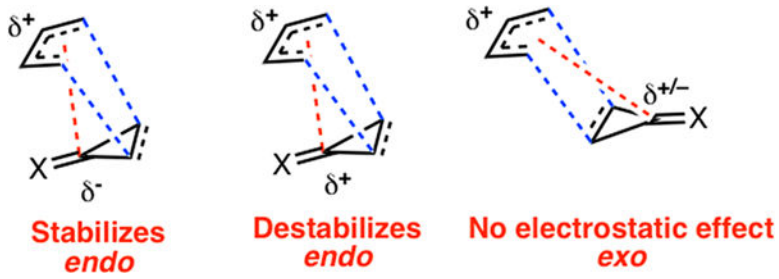

Figure 9.

Charge transfer in the *endo* and *exo* transition structures for the Diels—Alder reactions of butadiene (**Bd**) with a generic triafulvene. The primary orbital interactions and charge transfer are represented by blue and red lines, respectively.

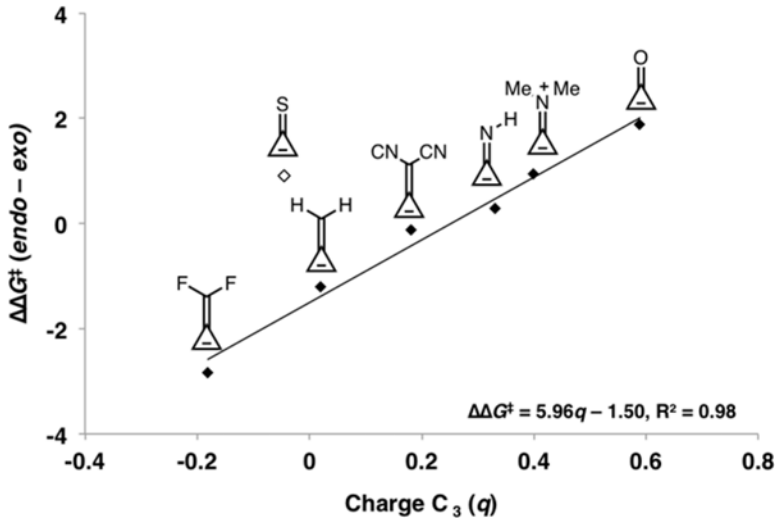

Figure 10.

Plot of the stereoselectivities measured as the difference in the activation free energies ($\Delta\Delta G^{\ddagger}$) between the endo and *exo* Diels− Alder reactions of triafulvenes 1−7 with butadiene (**Bd**) versus the computed NBO charge at C_3 in the triafulvene ground state.

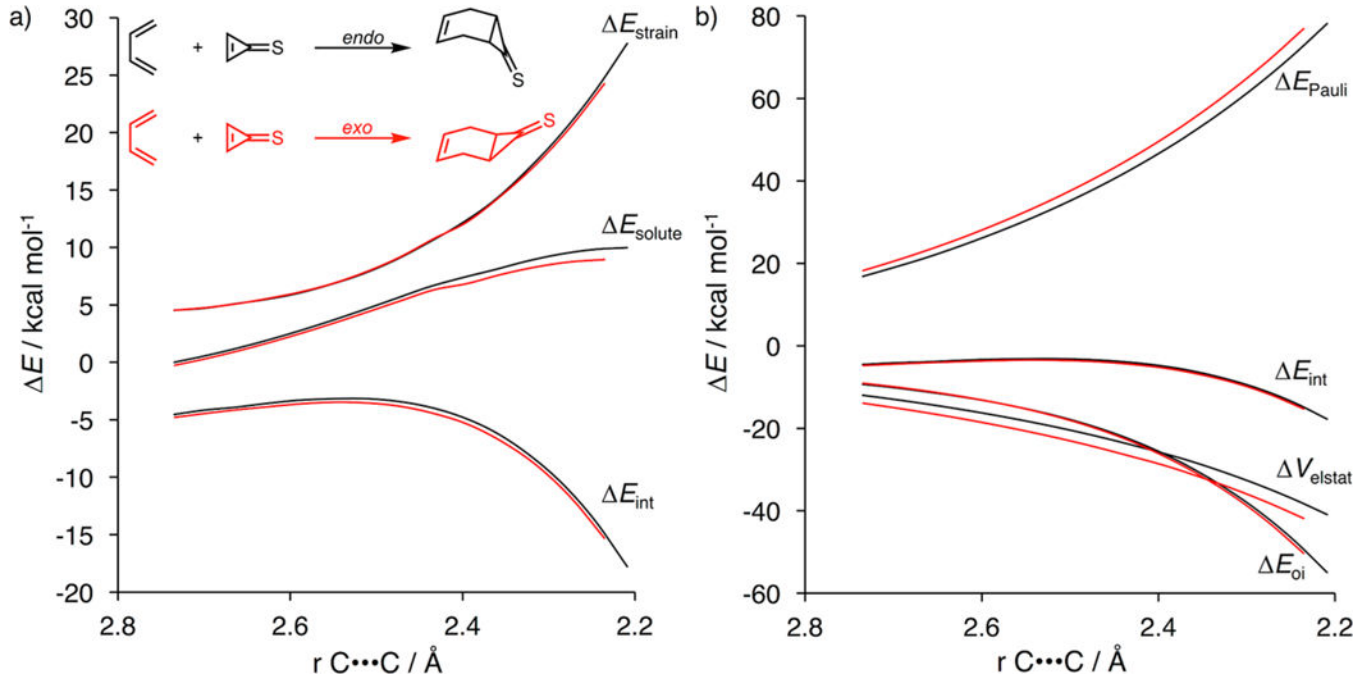

Figure 11.

(a) Distortion/interaction-activation strain analyses and (b) energy decomposition analyses for the *endo* (black) and *exo* (red) Diels—Alder reactions of butadiene (**Bd**) with cyclopropenethione (2).

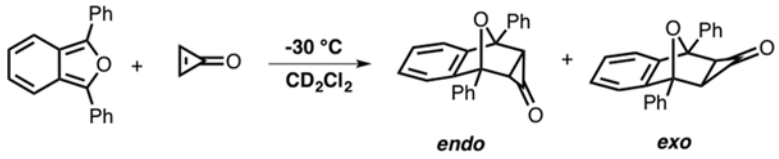

Scheme 1.

Diels—Alder Reaction of Cyclopropenone and 1,3-Diphenylisobenzofuran

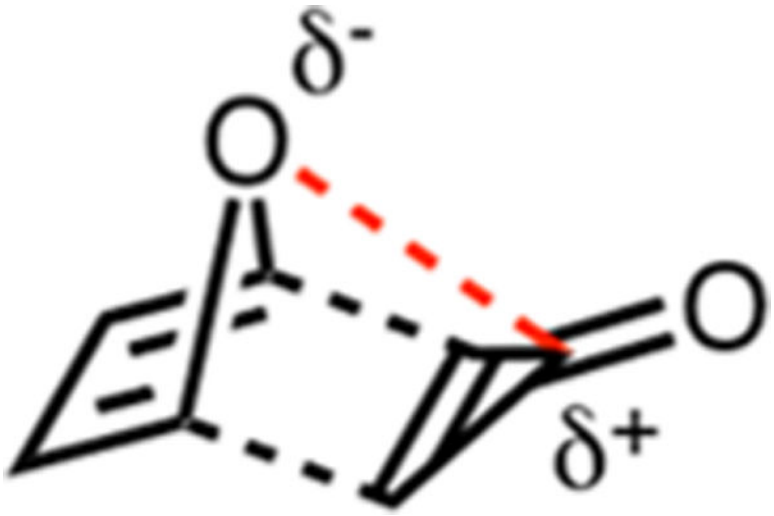

Scheme 2.

Stabilizing Electrostatic Interaction Proposed by Bachrach in the *Exo* Transition State for the Diels-Alder Reaction of Furan with Cyclopropenone[3]

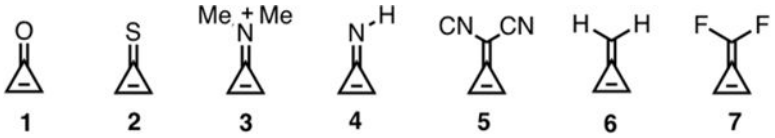

Scheme 3.
Cyclopropenone (l) and Analogs (2—7)